Cancer Research

Activation of the c-Met Pathway Mobilizes an Inflammatory Network in the Brain Microenvironment to Promote Brain Metastasis of Breast Cancer

Fei Xing[1], Yin Liu[1], Sambad Sharma[1], Kerui Wu[1], Michael D. Chan[2], Hui-Wen Lo[1], Richard L. Carpenter[1], Linda J. Metheny-Barlow[2], Xiaobo Zhou[3], Shadi A. Qasem[4], Boris Pasche[1], and Kounosuke Watabe[1]

Abstract

Brain metastasis is one of the chief causes of mortality in breast cancer patients, but the mechanisms that drive this process remain poorly understood. Here, we report that brain metastatic cells expressing high levels of c-Met promote the metastatic process via inflammatory cytokine upregulation and vascular reprogramming. Activated c-Met signaling promoted adhesion of tumor cells to brain endothelial cells and enhanced neovascularization by inducing the secretion of IL8 and CXCL1. Additionally, stimulation of IL1β secretion by activation of c-Met induced tumor-associated astrocytes to secrete the c-Met ligand HGF. Thus, a feed-forward mechanism of cytokine release initiated and sustained by c-Met fed a vicious cycle that generated a favorable microenvironment for metastatic cells. Reinforcing our results, we found that pterostilbene, a compound that penetrates the blood–brain barrier, could suppress brain metastasis by targeting c-Met signaling. These findings suggest a potential utility of this natural compound for chemoprevention. *Cancer Res; 76(17); 4970–80. ©2016 AACR.*

Introduction

Brain metastases of solid tumors are the most common central nervous system (CNS) malignancy with an incidence of 10-fold higher than primary brain tumors (1). Metastatic diseases contribute to over 90% of breast cancer deaths, and brain is one of the most lethal metastatic sites (2, 3). Even with the advanced treatment such as stereotactic radiosurgery, the median survival of breast cancer patients who developed brain metastases is around a year (4). Breast tumor is heterogeneous and classified into four major subtypes, and brain metastases are more prevalent in patients with the triple negative ($ER^-PR^-Her2^-$) and the $Her2^+$ subtype (5).

Based on clinical observation and the results of animal experiments, metastatic tumor cells are known to be disseminated in the brain at various stages of cancer progression, and some cells eventually recur when all the conditions of microenvironment are established (6). However, breast cancer patients often have a relative long period of remission before the diagnosis of brain metastases than other distant metastases, indicating that most tumor cells are either eliminated or remained dormant in the brain right after the extravasation (1). According to the "seed and soil" theory, only the cells that are able to adapt themselves to the new environment in distant organs can survive and thrive (7). Several lines of evidence indicate that establishing the perivascular growth by attaching to brain endothelial cells is essential to the early survival of brain metastatic cells (8, 9). After triggering the survival signaling by interacting with brain endothelial cells, tumor cells need to co-opt with the existing blood vessels and also to generate a network of blood vessels in order to support their further growth that requires the secretion of angiogenic promoting factors.

Astrocytes are the most abundant glial cells in the brain, and both tumor suppressing and promoting roles of astrocytes in brain metastases have been reported (8, 10). Astrocytes are present at the brain metastatic lesions even at the early stage of colonization, and they are mobilized to eliminate those cancer cells by secreting plasminogen activator, which induces FasL-mediated cell death and blocks vascular co-option by targeting L1CAM (8). On the other hand, astrocytes are also frequently observed in the macrometastasis lesions as tumor-associated astrocytes (TAA; ref. 11). We also previously demonstrated that physical contact between astrocytes and tumor cells enhanced the stemness of cancer stem like cells through the activation of the Notch pathway (12). Therefore, cancer cells must acquire two key properties to establish the metastatic growth in the brain; the abilities to overcome the tumor killing effects by the glial cells and

[1]Department of Cancer Biology, Wake Forest University School of Medicine, Winston-Salem, North Carolina. [2]Department of Radiation Oncology, Wake Forest University School of Medicine, Winston-Salem, North Carolina. [3]Department of Radiology, Wake Forest University School of Medicine, Winston-Salem, North Carolina. [4]Department of Pathology, Wake Forest University School of Medicine, Winston-Salem, North Carolina.

Note: Supplementary data for this article are available at Cancer Research Online (http://cancerres.aacrjournals.org/).

Corresponding Authors: Kounosuke Watabe, Department of Cancer Biology, Wake Forest University School of Medicine, Winston Salem, NC 27157. Phone: 336-716-0231; Fax: 336-716-0255; E-mail: kwatabe@wakehealth.edu and Fei Xing, Phone: 336-716-9576, fxing@wakehealth.edu

doi: 10.1158/0008-5472.CAN-15-3541

to create a suitable environment for further growth by communicating with the brain microenvironmental cells.

The antitumor efficacies of natural compounds have been extensively studied in many types of cancers (13). Interestingly, many natural compounds are known to be blood–brain barrier (BBB) penetrable, which makes them ideal candidates for treating CNS tumors, including brain metastases (14). In this study, we discovered a paracrine cytokine loop between TAAs and cancer cells, which continuously activates the c-Met pathway in cancer cells, followed by inducing angiogenesis in the metastatic site. Importantly, suppression of c-Met by the BBB-permeable natural compound, pterostilbene (PTER), significantly reduced the metastatic growth of cancer cells in the brain, suggesting the potential utility of PTER for intervention of breast cancer.

Materials and Methods

Cell culture and reagents

Human breast carcinoma cell lines SKBR3, MCF7, MDA-MB453 (MDA453), and MDA-MB231 (MDA231) were purchased from American Type Culture Collection. MDA-MB231BrM2a (231BrM), PC9, and PC9-BrM3 were kind gifts from Dr. Massague (Memorial Sloan-Kettering Cancer Center). 231HM was provided by Dr. Emily Wang (City of Hope). SKBrM3, 231BrM, and 231HM are brain metastatic cell lines derived from parental SKBR3 and MDA-MB-231 cells through several rounds of *in vivo* selections. Normal human primary astrocytes, human brain microvascular endothelial cells (HBMEC), and human umbilical vein endothelial cells (HUVEC) were purchased from Lonza. All cell lines were obtained between 2010 and 2014, and they were authenticated by qRT-PCR analysis for the expression of 20 signature genes. Culture conditions are described in the Supplementary Data.

Animal experiments

All animal experiments were done in accordance with a protocol approved by the Wake Forest Institutional Animal Care and Use Committee. For xenograft models, 10 nude mice [NU(NCr)-Foxn1^{nu}] in each group were injected with 10^5 luciferase-labeled tumor cells in 50% of Matrigel in a total volume of 100 μL. For experimental metastasis assay, 10 nude mice (7–8 weeks) in each group were injected with 2×10^5 luciferase-labeled cancer cells in PBS into left cardiac ventricle in a total volume of 100 μL.

Tube formation assays

A 96-well plate was coated with 50-μL growth factor-reduced Matrigel (BD) until it was solidified at 37°C. HBMECs (2×10^4 cells) were suspended in EGM-2 growth medium or serum-free conditioned medium from cancer cells, and they were seeded on top the growth factor-reduced Matrigel. After 6 hours, photos were taken under a microscope, and the number of tubes structures per filed was counted.

Gene Set Enrichment Analysis

The Gene MatriX file (.gmx) was generated by combining the top 200 downregulated genes when MCF7 cells were treated with pathway specific inhibitors (GSE31912) and also by adopting oncogenic signatures that were deposited in Molecular Signatures Database (MsigDB; ref. 15). We also expanded the TKR signature genes that were not available from the previous two data sets and these include FGF (GSE17916), TrkA (GSE18409), Axl (GSE30543), EphB2 (GSE66361), Ret (GSE41405), and c-Met (E-MTAB-762) pathways (16). The complete list of signatures is shown in Supplementary Table S1. Gene Cluster Text file (.gct) was generated from four breast cancer cohorts (GSE2034, GSE2603, GSE5327, GSE12276, and GSE14020), normalized by MAS5.0 and centered to the median of all probes. Categorical class file (.cls) was generated based on the brain metastasis status of each patient. The number of permutations was set to 1,000, and we used HG_U133A_2 as the chip platform.

All other routine methods are described in Supplementary Materials and Methods.

Results

c-Met pathway is enriched in patients with brain metastases

To identify pathological pathways that promote the progression of brain metastases, we developed a novel screening approach by first generating a set of signature genes that covers 83 oncogenic pathways (Supplementary Table S1). The detailed approach for generating the signatures is described in Experimental Procedures. We then tested these signature genes on a patient cohort data containing a total of 710 breast cancer patients, of which 47 subjects developed brain metastases over a period of 12 years (Supplementary Table S2). The tumor subtype information was published in a previous study (17). We performed Gene Set Enrichment Analysis (GSEA) and the brain metastasis-free survival analysis to identify the pathways that are specifically enriched in patients with brain metastases (Fig. 1A and Supplementary Table S3). The results of GSEA indicate that the c-Met pathway, a potent tyrosine kinase receptor signaling that affects the growth, migration, and invasion of cancer cells, is the only significantly enriched pathway among 83 pathways in the patients with brain metastases but not with bone metastases compared with the metastasis-free patients (Fig. 1B and Supplementary Fig. S1). To further validate the results, we created another c-Met signature using 300 most upregulated genes by hepatocellular growth factor (HGF) in Madin-Darby canine kidney (MDCK) cells, and found that this signature was also significantly enriched in patients with brain metastases (Fig. 1C). The brain metastasis-free survival analysis also indicate that patients with a higher level of c-Met in their primary tumors rapidly developed brain metastases but not bone metastases, suggesting that the c-Met pathway preferentially promotes brain metastases (Fig. 1D). Notably, the c-Met gene was found to be significantly overexpressed in the brain metastatic lesions compared with metastatic tumors in the other sites, suggesting that activation of the c-Met pathway may be due to the brain tumor microenvironment (Fig. 1E). Therefore, based on the results of our GSEA and brain metastasis-free survival analyses, we decided to focus on the c-Met pathway whose activation and function during the progression of brain metastases are still poorly understood.

c-Met overexpression is associated with aggressive phenotype of brain metastases

Because the basis of GSEA and survival analysis rely on the expression profile of mRNA instead of protein, we examined the total c-Met protein level in clinical samples derived from primary tumors with or without brain metastases and tumors from brain metastatic lesions. We found that, primary tumors derived from

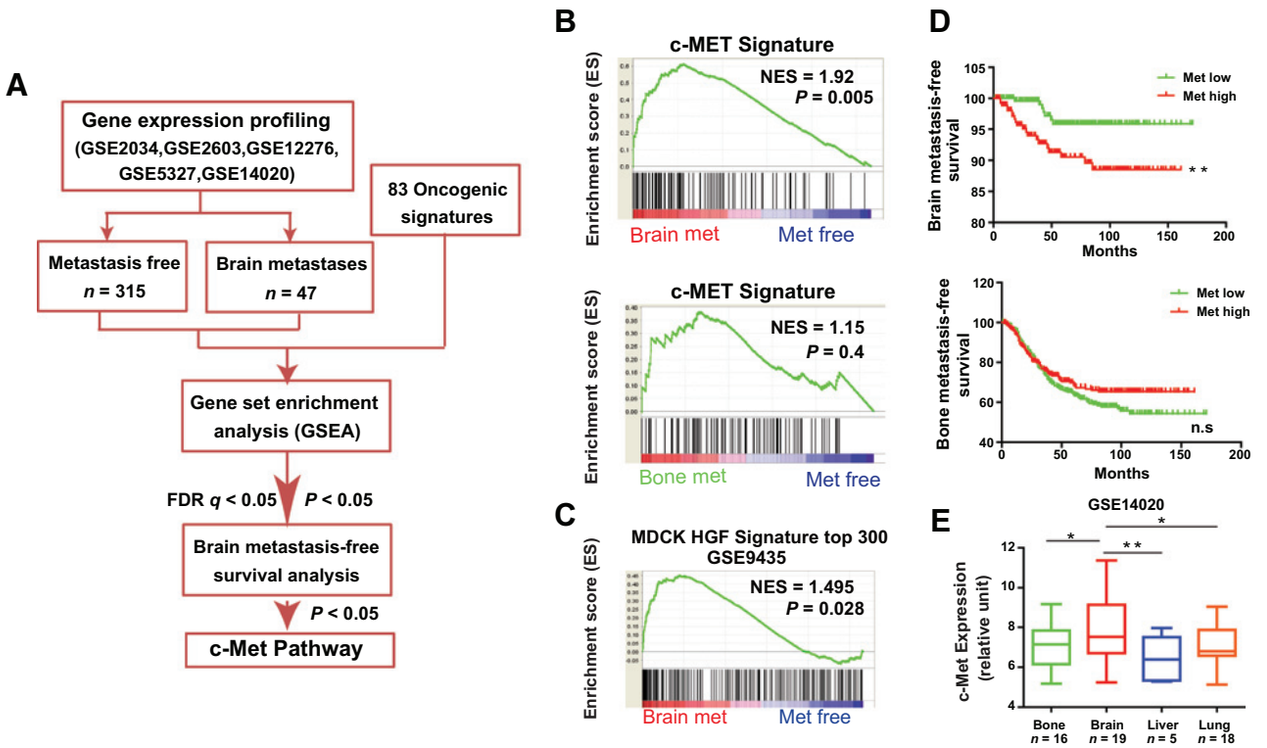

Figure 1.

c-Met signaling is enriched in breast cancer patients with brain metastases. **A,** a work flowchart for identifying key regulatory pathways related to breast cancer brain metastasis by using GSEA followed by brain metastasis-free survival analyses. **B,** GSEA enrichment charts of c-Met signature genes in patients with brain metastases (top) and bone metastases (bottom) compared with metastasis-free patients. **C,** GSEA enrichment chart of HGF signature genes in patients with brain metastases compared with metastasis-free patients. The HGF signature genes were derived from MDCK cells treated with HGF (GSE9435). **D,** brain (top) and bone (bottom) metastasis-free survival analysis for the c-Met gene in the combined cohort used in **A**. **E,** c-Met expressions in different metastatic sites were compared using GSE14020. *, $P < 0.05$; **, $P < 0.001$.

patients with brain metastases and tumors from brain metastatic lesions expressed higher level of c-Met protein than the tumors from metastasis-free patients (Fig. 2A). Notably, no significant difference of c-Met expression was found between primary tumor with brain metastases and tumors isolated from brain metastatic lesions, in both our immunohistochemical and gene expression analyses (Supplementary Fig. S2A). In addition, a strong activation of the c-Met pathway in brain metastatic lesions was observed by staining with phospho-c-Met antibody (Supplementary Fig. S2B). These results strongly suggest the c-Met expression in primary tumors as a potential prognostic marker to predict the progression of brain metastases. To establish the suitable brain metastatic models that recapitulate the clinical features, we first examined the c-Met mRNA expression levels in various breast cancer cell lines using a published database (GSE10843). Interestingly, we found that triple-negative breast cancer cells (ER^-, PR^-, $HER2^-$) that are known to metastasize to the brain more efficiently than other subtypes expressed a significantly higher amount of c-Met (Fig. 2B). Our results of GSEA also confirmed that c-Met signature genes were highly enriched in triple-negative breast cancer patients (Fig. 2C). We also found that c-Met was highly expressed in the triple-negative primary tumors derived from patients with brain metastases (Supplementary Fig. S2C). MDA-MB-231 (MDA231) is a triple-negative cell line isolated from a breast cancer patient with metastatic diseases. Two groups generated 231BrM2a (231BrM) and 231HM, which preferentially metastasize to the brain from the parental MDA231 cells by several rounds of intracardiac and orthotopic injection, respectively. We also established another brain metastatic cell line, SKBrM3. The brain metastatic capability of SKBrM3 and parental SKBR3 was confirmed *in vivo* (Supplementary Fig. S2D). The results of c-Met Western blot demonstrated that these brain metastatic variants expressed a much higher level of c-Met than their parental cells, which is consistent with our IHC results (Fig. 2D). c-Met was also found to be overexpressed in the PC9BrM3 cells, a brain metastatic variant derived from a non–small cell lung carcinoma cell line PC9, suggesting that c-Met expression is associated with brain metastases in multiple types of cancers (Supplementary Fig. S2E). To elucidate the exact role of the c-Met pathway in the progression of brain metastases, we generated two cell lines carrying the doxycycline-inducible sh-c-Met transgene from 231BrM and SKBrM3 cells (Fig. 2E and Supplementary Fig. S2F). Next, we intracardially inoculated 231BrM/Dox/sh-c-Met cells into nude mice followed by inducing the expression of shRNA targeting c-Met at day1 or day7. As shown in Fig. 2F, knockdown of c-Met significantly suppressed the growth of tumor cells with an increased brain metastasis-free survival. Interestingly, early knockdown of c-Met right after the inoculation (day 1) significantly reduced the tumor growth rate and brain metastasis incidence compared to the delayed induction (day 7), indicating

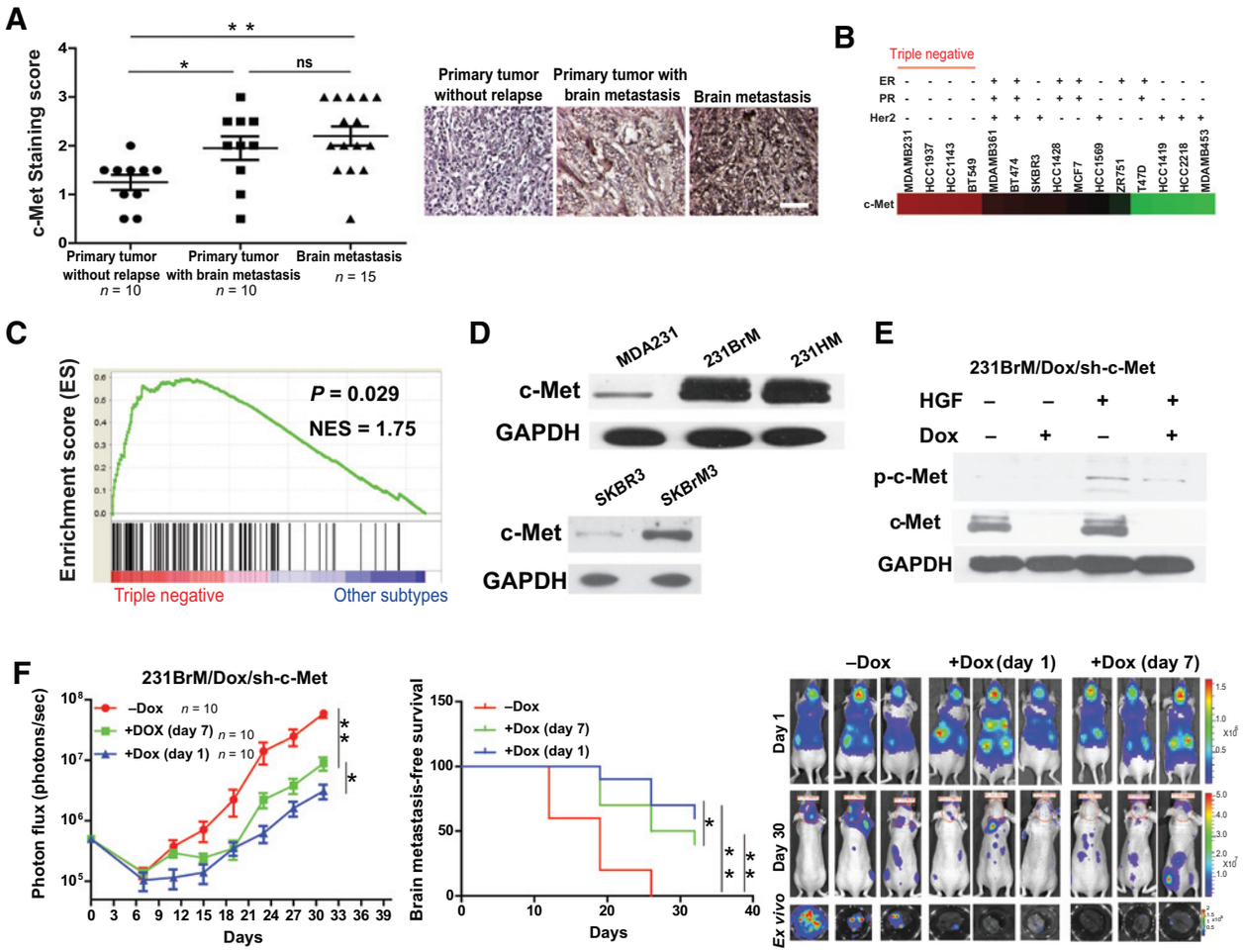

Figure 2.

c-Met is highly expressed in triple-negative breast cancer cells and promotes brain metastasis *in vivo*. **A,** immunohistochemical quantification of c-Met protein expressions in samples from primary tumors with or without brain metastases and samples derived from brain metastatic lesions (left). Right, representative photos of c-Met staining. Scale bars, 50 μm. **B,** heatmap analysis of c-Met expression in different subtypes of breast cancer cell lines using the GSE10843 database. **C,** GSEA enrichment chart of c-Met signature genes between triple-negative breast cancer patients ($n = 140$) and patients with other subtypes ($n = 570$). **D,** anti-c-Met Western blot analysis for c-Met of brain metastatic cells and their parental cells. **E,** Western blot analyses for total and phospho c-Met proteins in 231BrM/Dox/sh-c-Met cells that were treated with or without HGF (20 ng/mL) and doxycycline (1 μg/mL). **F,** 231BrM/Dox/sh-c-Met (2×10^5 cells) were intracardially injected into nude mice ($n = 10$) followed by giving them with doxycycline in drinking water at different time points (day 1 or day 7). Left, total photon flux of brain metastatic lesions was measured by BLI at the time indicated. Middle, Kaplan–Meier analysis for brain metastasis-free survival of mice fed with the indicated water. Right, BLI images of brain metastatic lesions of three representative mice from each experimental group.

that the c-Met pathway is crucial for the early seeding of metastatic cells. Notably, knockdown of c-Met suppressed tumor growth in culture by 20%, and by four times in a xenograft model (Supplementary Fig. S2G and S2H). However, the degree of inhibition was significantly more profound in the experimental metastasis model as shown in Fig. 2F, indicating that brain metastatic cells are more dependent on the c-Met signaling for their survival and growth in the brain.

Knockdown of c-Met gene suppresses multiple brain metastasis–associated cytokines

To elucidate the molecular mechanisms by which c-Met pathway activation leads to brain metastasis, we performed genome-wide gene profiling (GSE25976) in 231BrM/Dox/sh-c-Met and SKBrM3/Dox/sh-c-Met with or without the knockdown of c-Met gene by doxycycline treatment (Fig. 3A). We found that five genes (BTF3L4, EPDR1, IL1B, CXCL1, and IL8) are significantly downregulated upon knockdown of c-Met in both cell lines. We then examined the relationship of these genes with brain metastasis-free survival of breast cancer patients using existing cohort data. Strikingly, the expression of three major inflammatory cytokine genes, IL1β, IL8, and CXCL1, was all significantly correlated to brain but not bone metastasis-free survival (Fig. 3B; Supplementary Fig. S3A). We then validated the result of profiling experiment by directly measuring mRNA and protein expression of IL1β, IL8, and CXCL1 in the same samples used in Fig. 3A (Fig. 3C; Supplementary Fig. S3B). Furthermore, the expressions of these three genes were found to

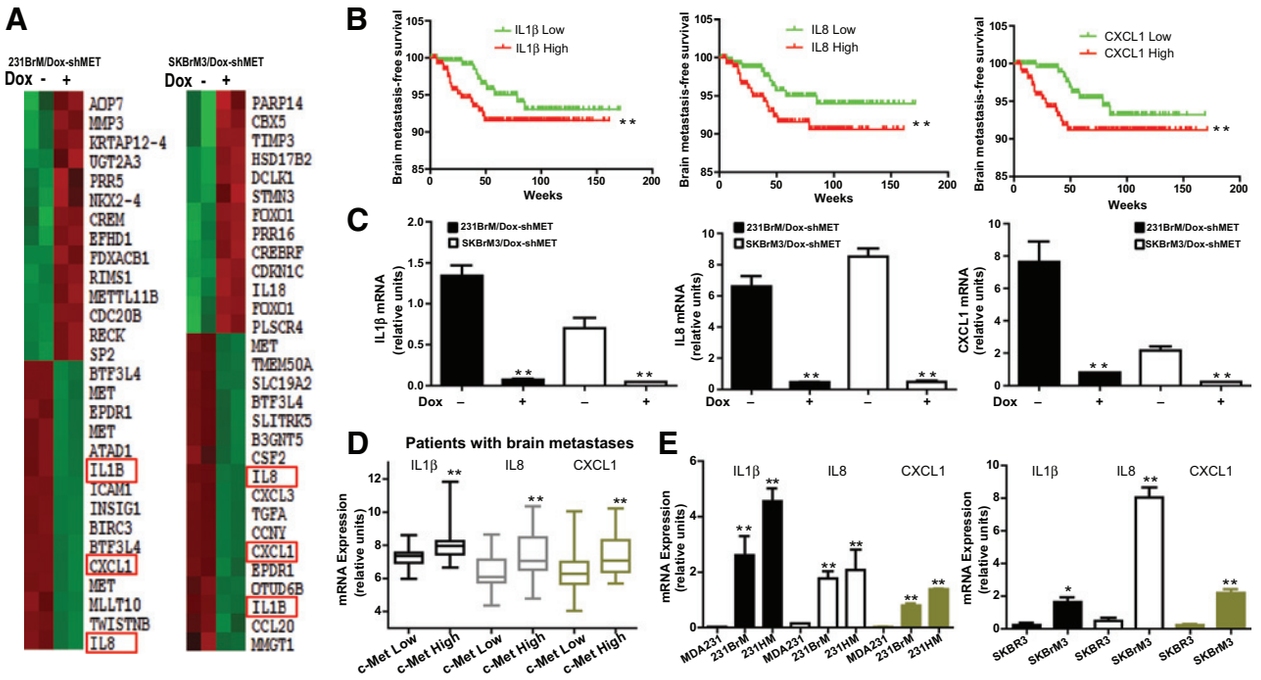

Figure 3.

Knockdown of c-Met suppresses IL1β, IL8, and CXCL1 expressions in brain metastatic cells. **A,** heat maps were generated with the genes that were significantly upregulated or downregulated in the 231BrM/Dox/sh-c-Met and SKBrM3/Dox/sh-c-Met cells that were treated with or without doxycycline. **B,** brain metastasis-free survival analyses of IL1β, IL8, and CXCL1 in 710 breast cancer patients using the combined GEO databases (GSE12276, GSE2034, GSE2603, GSE5327, and GSE14020). Patients were divided into two groups based on the expression status of gene in their primary tumors. **C,** qRT-PCR analyses for IL1β, IL8, and CXCL1 of the indicated cells with or without the treatment of doxycycline. **D,** box whisker analyses of IL1β, IL8, and CXCL1 expressions in c-Met^{low} and c-Met^{high} groups of patients who developed brain metastases. **E,** mRNA levels of the indicated genes in the parental MDA231 (left) and SKBR3(right) cell lines and their brain metastatic variant cells (231BrM, 231HM, and SKBrM3).

be positively correlated with c-Met expression in patients with brain metastases (Fig. 3D). Our results of qRT-PCR and ELISA analyses also demonstrated that all of three genes were highly expressed in brain metastatic variant cell lines compared with the parental cells, suggesting that the brain metastatic cells are more inflammatory and they are able to trigger a broad cytokine response from the surrounding microenvironment. (Fig. 3E; Supplementary Fig. S3C).

c-Met–MAPK–IL1β axis promotes chemokine release in brain metastatic cells

To clarify the pathways that mediate the release of these three inflammatory cytokines by c-Met, we ectopically expressed the c-Met gene in two c-Met^{low} cell lines, MCF7 and MDA-MB453, followed by examining the expressions of IL1β, IL8, and CXCL1. We found that IL1β, IL8, and CXCL1 were indeed significantly upregulated by ectopic expression of c-Met in both MDA453/Met and MCF7/Met cells (Fig. 4A). We also generated an MDA453 line that expresses c-Met under the control of doxycycline, and all of these three genes were found to be significantly augmented by the induction of c-Met (Supplementary Fig. S4A). Consistent with these results, only moderate induction of these factors was observed in c-Met^{low} cells after the treatment of HGF (Supplementary Fig. S4B). Because IL1β is known to promote IL8 and CXCL1 expression in several types of immune cells, we therefore postulated that the induction of IL8 and CXCL1 by c-Met is mediated by IL1β. We then analyzed the correlation between c-Met and these three genes in breast tumors and found that only IL1β is positively correlated with c-Met in patients with brain metastases but not with bone or lung metastases, suggesting that IL1β is the immediate responding gene of c-Met activation (Fig. 4B; Supplementary Fig. S4C and S4D). MAPK, PI3K/AKT, and STAT3 have been identified as the major transducers of c-Met signaling (18). To identify the exact pathway involved in the induction of IL1β by c-Met, pathway-specific inhibitors were added in the culture of MDA453/Met, 231BrM and SKBrM3 cells followed by examining the IL1β expression. As shown in Fig. 4C, IL1β levels were significantly decreased in all of three cell lines after treating the cells with PD98059, a MAPK-specific inhibitor. We also observed a significant decrease in IL8 and CXCL1 expressions in 231BrM with a stable expression of shRNA that was targeted to IL1β (Fig. 4D). On the other hand, recombinant IL1β induced nearly a 10-fold increase of IL8 and CXCL1 mRNA in MCF7 and MDA453 cells (Fig. 4E). These results indicate that the MAPK pathway is the major downstream transducer between c-Met and IL1β whose expression lead to the secretion of IL8 and CXCL1.

c-Met activation enhances perivascular adhesion and angiogenesis through IL8- and CXCL1-mediated CXCR1 signaling

The survival and growth of metastatic tumor cells in the brain is known to require a support of blood vessel and

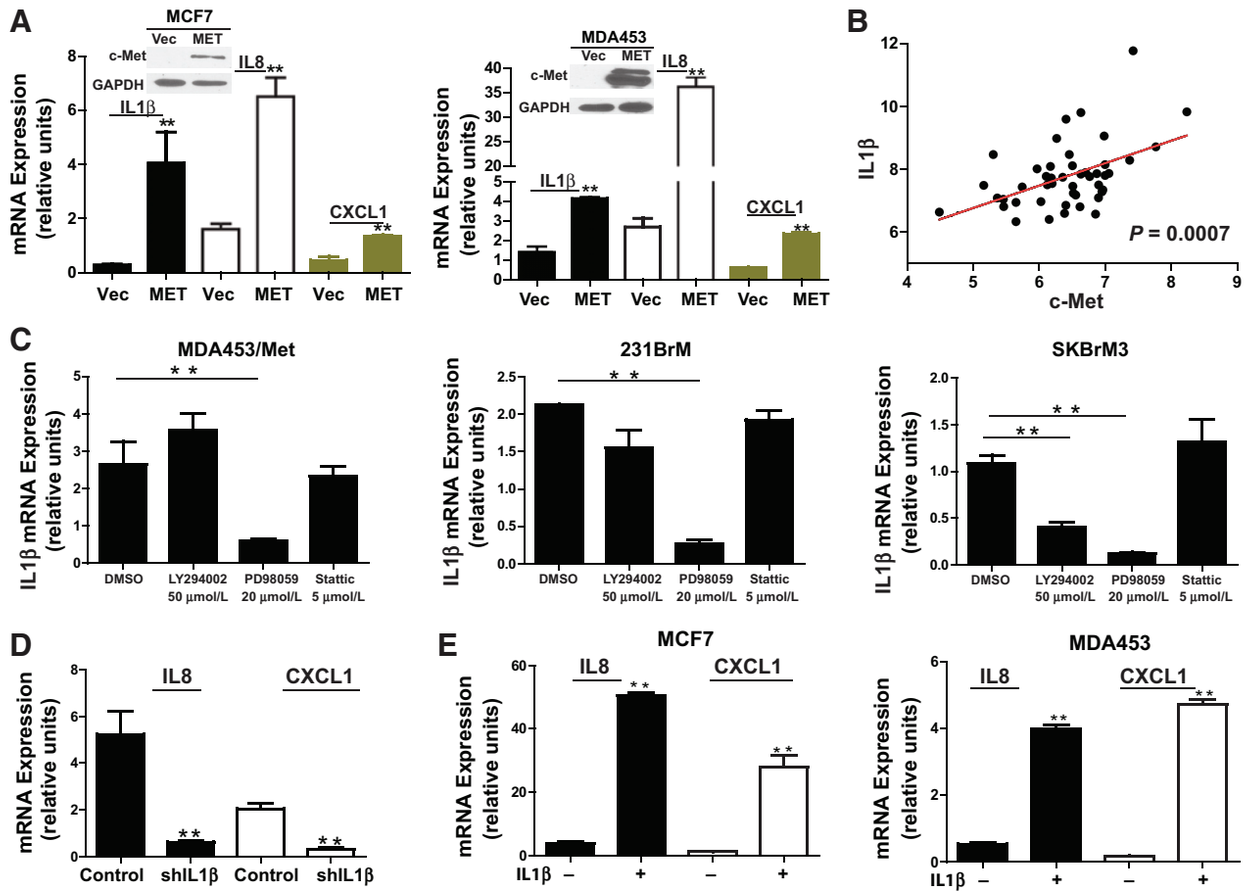

Figure 4.

c-Met signaling induces IL1β, IL8, and CXCL1 through the MAPK pathway. **A,** qRT-PCR analyses for IL1β, IL8, and CXCL1 mRNA levels in MCF7 (left) and MDA453 (right) cells with or without ectopic expression of c-Met. Western blot analyses of c-Met are shown in the insets. **B,** correlation of IL1β and c-Met mRNA expression in a total of 47 breast cancer patients with brain metastases. **C,** cancer cells were treated with different pathway inhibitors followed by measuring of mRNA levels of IL1β. **D,** mRNA levels of IL8 and CXCL1 were measured for 231BrM cells with or without knockdown of IL1β by shRNA. **E,** qRT-PCR analysis of mRNA expression in MCF7 (left) and MDA453 (right) cells that were treated with or without recombinant IL1β.

perivascular niche rather than growing solitarily (19). Our *in vivo* results also suggest that c-Met signaling is crucial in the early progression of cancer cells in the brain, and suppressing the c-Met at the time of colonization significantly impairs the growth rate of cancer cells. To investigate the role of c-Met signaling in the perivascular growth of cancer cells, we first tested the adhesion ability of cancer cells to HBMECs. Green fluorescent dye-labeled tumor cells carrying the doxycycline-inducible sh-c-Met were treated with or without doxycycline for 48 hours to knock down the c-Met expression followed by seeding them on top of the HBMECs. As shown in Fig. 5A, the number of tumor cells attached to HBMEC was significantly decreased in the c-Met knockdown group compared with the control, suggesting that the c-Met signaling may contribute to the adhesion of cancer cells to blood vessels for early colonization. To further validate this notion, we used the endothelial cell tubular forming model, which mimics the initial step of vescularization. HBMECs were labeled with red fluorescent dye and seeded on Matrigel to form tube-like structures. We then added GFP-labeled tumor cells on top of the tube structures followed by examining attachment of cancer cells to HBMECs. As shown in Fig. 5B, the knockdown of c-Met blocked the interaction between cancer cells and HBMECs, which is consistent with the result of the monolayer binding assays. The direct interaction of tumor cells and endothelial cells at perivascular niche is believed to be a reciprocal action, and tumor cells need to support angiogenesis for their own growth. Because IL8 and CXCL1 were previously identified as key angiogenic factors in various types of tumors, we hypothesized that c-Met-mediated induction of IL8 and CXCL1 enhances the angiogenesis in brain metastatic lesions. To test this hypothesis, HBMECs were cultured in the conditioned medium (CM) derived from cancer cells, and their tube formation ability was examined to measure the angiogenic activity. We found that the tube-forming ability of HBMECs was significantly elevated when they were cultured in the CM derived from brain metastatic cells compared with the CM of parental cells. Importantly, this effect was significantly suppressed by treating cells with repertaxin, a specific inhibitor of CXCR1, which is the major receptor of IL8 and CXCL1 (Fig. 5C). We also examined

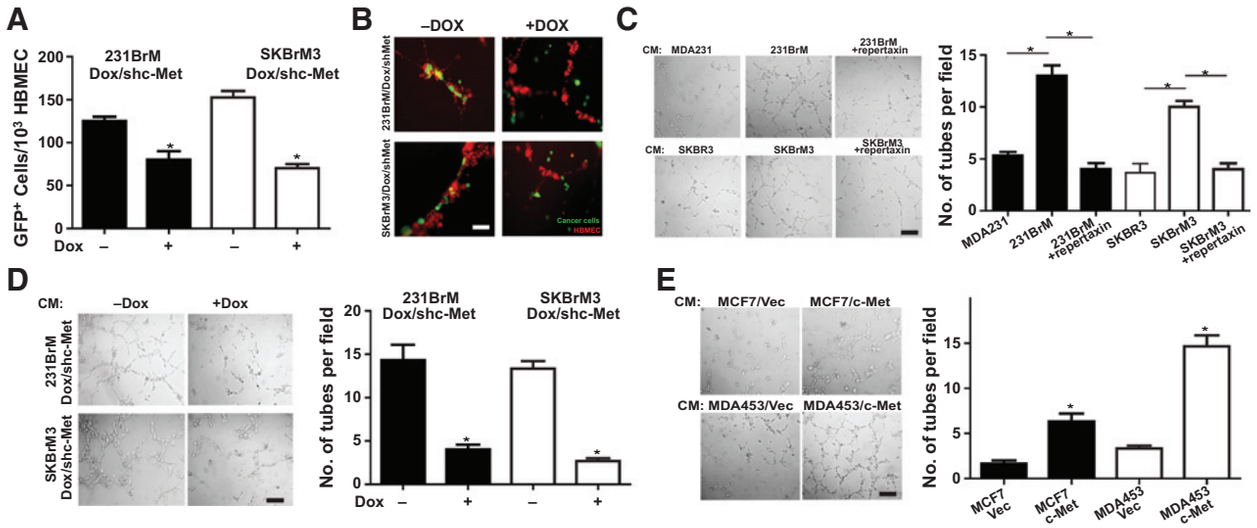

Figure 5.

c-Met signaling promotes perivascular growth and angiogenesis of cancer cells. **A,** 231BrM/Dox/sh-c-Met and SKBrM3/Dox/sh-c-Met cells were treated with or without doxycycline to induce knockdown of c-Met for 48 hours and the cells were seeded on top of HBMECs. Cells were washed with PBS and the number of attached GFP^+ tumor cells were counted under a fluorescent microscope. **B,** HBMECs (2×10^4) were labeled with red cell tracker dye and seeded on top of the Matrigel for 6 hours to form the tube-like structure. A total of 5×10^3 tumor cells labeled with the green cell tracker dye was treated with or without doxycycline for 48 hours and they were seeded on top of the HBMECs. Photos were taken after 6 hours incubation. Scale bars, 20 μm. **C,** 2×10^4 HBMECs were incubated in the indicated conditioned medium with or without 10 mmol/L repertaxin for 6 hours followed by measuring their tube-forming abilities. **D,** 2×10^4 HBMECs were incubated in the conditioned medium prepared from 231BrM/Dox/sh-c-Met and SKBrM3/Dox/sh-c-Met cells with or without the treatment of doxycycline. Photos were taken after 6 hours of incubation followed by measuring the tube-forming ability of HBMECs. **E,** 2×10^4 HBMECs were incubated with the conditioned medium prepared from MCF7 or MDA453 with or without ectopic expression of c-Met. Photos were taken after 6 hours incubation followed by measuring the tube-forming ability of HBMECs. Scale bars, 100 μm.

the endothelial cell proliferation after incubating the cells for 48 hours in the presence of IL8 or CXCL1 and found that only CXCL1 was able to slightly but significantly (by 25%) promote proliferation of brain endothelial cells (Supplementary Fig. S5). These results indicate that the ability of tube formation is independent on the growth of endothelial cells. We also tested CM derived from cells with knockdown or overexpression of c-Met in the brain metastatic cells and $c\text{-Met}^{low}$ nonmetastatic cells, and found that these cells significantly reduced or enhanced the tube-forming ability of HBMECs, respectively (Fig. 5D and E).

c-Met–induced IL1β promotes HGF secretion from TAAs

The activation of canonical c-Met signaling requires the presence of HGF, which is mainly secreted by noncancerous stromal cells, and our previous studies demonstrated that TAAs are actively involved in the metastatic growth in the brain (12). By analyzing the samples derived from brain metastatic lesions of breast cancer patients, we found that a group of cancer cells that were located adjacent to the GFAP-positive TAAs showed strong activation of c-Met signaling, suggesting that TAAs may be a potential source of HGF (Fig. 6A). To examine whether secretary factors from tumor cells regulate the HGF expression in TAAs, we treated primary human astrocytes with various CM from different cancer cell lines and found that only CM derived from brain metastatic cell line were able to induce HGF expression in astrocytes (Fig. 6B). Our immunocytochemistry results also indicate that the astrocytes that were treated with CM of brain metastatic cells expressed a much higher level of both GFAP and HGF compared with the control cells (Fig. 6C). We also examined HGF and GFAP expressions in the TAAs surrounding a brain metastatic lesion in the mice and found that TAAs express a much higher level of HGF compared with the tumor cells (Fig. 6D). In addition, the result of our Taqman qPCR using species-specific primers indicated that tumor cells are the major source of IL1β, IL8, and CXCL1 (Supplementary Fig. S6A). To further examine the cross-talk between brain metastatic cells and TAAs, we established a Transwell-based coculture model. When cancer cells and astrocytes were cocultured in this system, HGF expression in astrocytes was significantly augmented by brain metastatic variants compared with parental cells (Fig. 6E). Next, we removed the cancer cells in the upper chamber membrane followed by measuring the level of c-Met activation in tumor cells by immunocytochemistry and Western blot (Fig. 6F). As shown in Fig. 6G and H, the coculture of tumor cells with astrocytes significantly induced c-Met activation and its downstream MAPK signaling in the brain metastatic cells. On the other hand, we found that GFAP expression in astrocytes was strongly elevated after coculturing with brain metastatic cells (Supplementary Fig. S6B). Because IL1β, IL8, and CXCL1 were the most upregulated factors by c-Met, we speculated that they may stimulate the secretion of HGF from astrocytes in addition to promoting angiogenesis. As shown in Fig. 6I, we found that IL1β was able to most significantly upregulate HGF expression in astrocytes compared with IL8 and CXCL1. Our result of immunocytochemistry also demonstrated that IL1β-treatment stimulated HGF

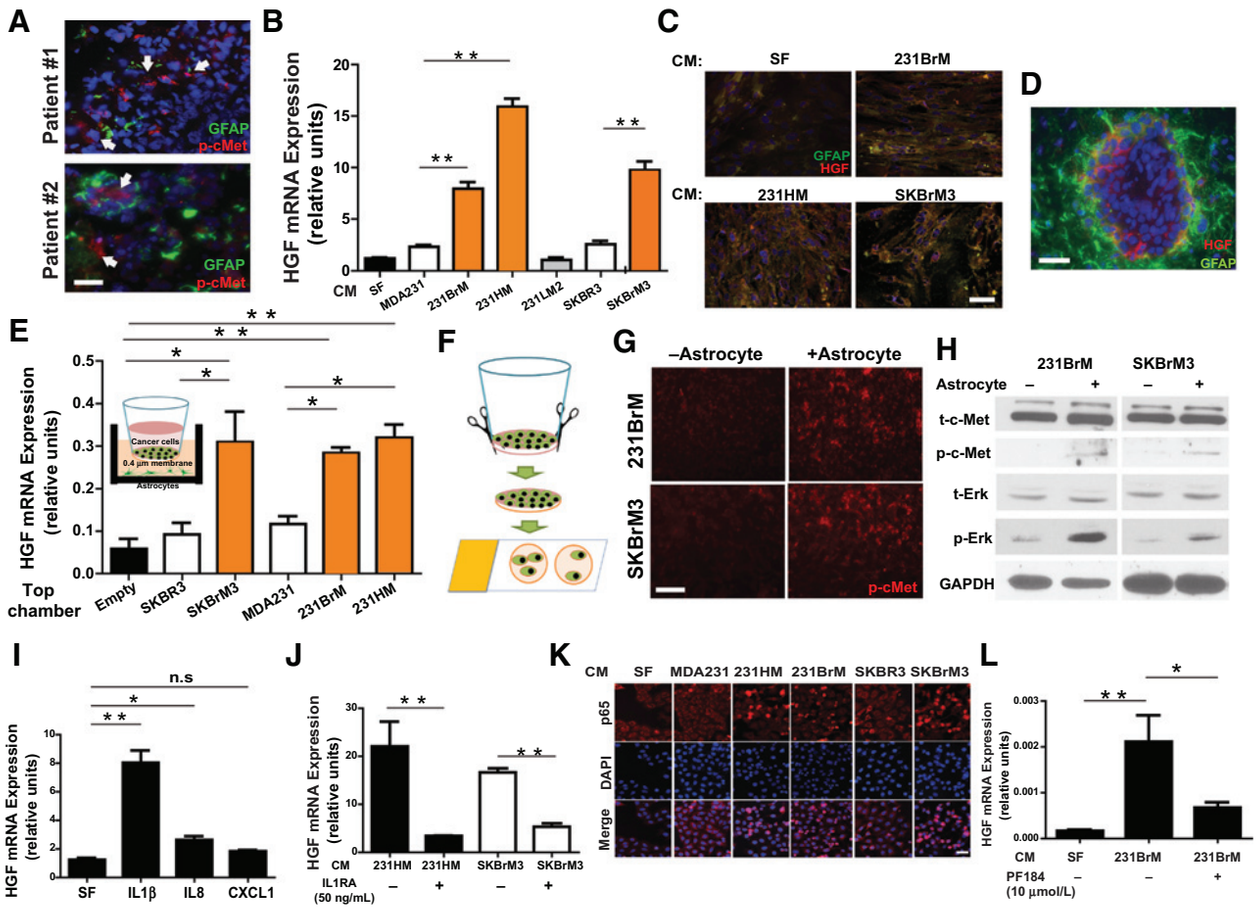

Figure 6.

c-Met–induced IL1β enhances HGF secretion from TAAs. **A,** immunocytochemical analysis of GFAP and phospho-c-Met expression in brain metastatic lesions from breast cancer patients. **B,** mRNA expression of HGF was measured in human normal astrocytes that were treated with the indicated conditioned medium from breast cancer cells. **C,** immunocytochemical analysis of GFAP and HGF expression in human normal astrocytes that were treated with the conditioned medium derived from brain metastatic cells. **D,** immunocytochemical analysis of GFAP and HGF expression for a brain metastatic lesion from a mouse inoculated with 231BrM cells. **E,** HGF expressions in human normal astrocytes with or without coculturing cancer cells were measured by qRT-PCR. Cancer cells were seeded in the upper chamber of a Transwell until they become confluent followed by coculturing with human normal astrocytes in the bottom chamber for 48 hours (inset). **F,** a cartoon showing preparation of the cancer cells for immunocytochemical analysis from the Transwell membrane. **G,** immunocytochemical analysis of c-Met phosphorylation in cancer cells that were cocultured with or without astrocytes as illustrated in **F**. **H,** the cancer cells grown on the Transwell membrane were collected and subjected to Western blot analyses with the indicated antibodies. **I,** mRNA levels of HGF in human normal astrocytes that were treated with the indicated recombinant proteins were measured by qRT-PCR after 48 hours of incubation. **J,** human normal astrocytes were treated with the indicated conditioned medium in the presence or absence of IL1RA (20 μg/mL) for 48 hours followed by measuring the mRNA levels of HGF by qRT-PCR. **K,** immunocytochemical analyses for nuclear localization of the p65 protein in human normal astrocytes that were treated with the indicated conditioned medium. **L,** human normal astrocytes were treated with 231BrM conditioned medium with or without the addition of the NF-κB inhibitor PF-184 for 48 hours followed by measuring the mRNA levels of HGF. Scale bars, 100 μm (**A, C, D**), 200 μm (**G**).

and GFAP expression in astrocytes (Supplementary Fig. S6C). Notably, blocking the IL1β signaling by IL1RA (IL1 receptor antagonist) significantly attenuated the induction of HGF in astrocytes that were treated with CM derived from the brain metastatic cell (Fig. 6J). Furthermore, because the NF-κB pathway is one of the major downstream effectors of IL1β signaling (20), we examined the expression of NF-κB components, P65 and P50, in astrocytes that were treated with CM of the brain metastatic cells. We found that both P65 and P50 were strongly localized in nucleus upon treatment of astrocytes by CM and that the expression of GFAP in these cells was also strongly increased (Fig. 6K; Supplementary Fig. S6D). To further validate these results, astrocytes were treated with brain metastatic CM with or without the presence of IKKβ inhibitor, PF184. We found that PF184 significantly abrogated the HGF expression induced by 231BrM CM (Fig. 6L). These results strongly suggest that IL1β upregulates HGF expression in astrocytes through activation of the NF-κB pathway.

PTER suppresses brain metastases by targeting c-Met

Dietary chemoprevention of metastatic tumor growth is one of the effective ways to delay the occurrence of distant

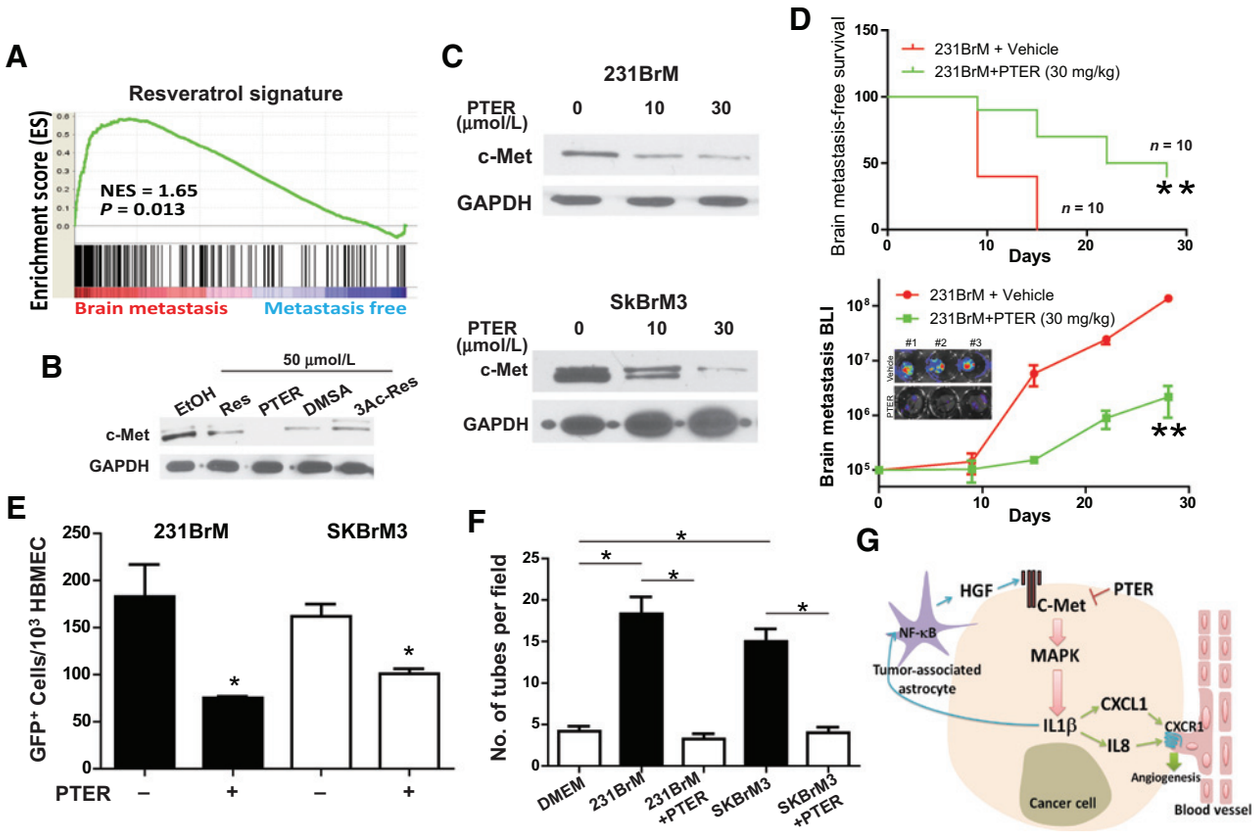

Figure 7.

Pterostilbene (PTER) suppresses brain metastasis by targeting c-Met. **A,** GSEA showing that the resveratrol signature genes were enriched in patients with brain metastases. **B,** Western blot analysis for c-Met expression in 231BrM cells that were treated with various resveratrol analogues. **C,** Western blot analysis for c-Met expression in 231BrM (top) and SKBrM3 (bottom) cells that were treated with various doses of PTER. **D,** luciferase-labeled 231BrM cells were intracardially injected into nude mice followed by delivering PTER (30 mg/kg) by i.p. injection every 2 days. $n = 10$ for each group. Top, Kaplan–Meier analysis for brain metastasis-free survival of mice treated with or without PTER. Bottom, total photon flux of brain metastatic lesions was measured by BLI at the indicated time. Brain *ex vivo* images of three representative mice are shown (inset). **E,** 231BrM and SKBrM3 cells were treated with 10 μmol/L PTER for 24 hours followed by accessing their binding abilities to HBMECs. **F,** tube formation assays of HBMECs after incubation with the conditioned medium from brain metastatic cells in the presence or absence of PTER (10 μmol/L). **G,** the model illustrates a c-Met–regulated inflammatory network in brain metastasis.

metastases (21). To identify potential natural compounds that can prevent or suppress brain metastases, we selected 9 BBB-permeable natural compounds for which expression prolife data in response to these compounds are available, and we performed the GSEA-based screening (Supplementary Fig. S7A). The result of GSEA indicated that a gene signature that was suppressed by resveratrol treatment was most significantly enriched in patients with brain metastases (Fig. 7A and Supplementary Table S4). We therefore obtained several resveratrol analogues that may be effective on suppressing brain metastasis (Supplementary Fig. S7B). We first examined whether these analogues can target c-Met, the key regulator of brain metastases found in this study. As shown in Fig. 7B, the c-Met level in 231BrM was indeed significantly decreased in the resveratrol-treated group. Interestingly, one of the resveratrol analogues, PTER, showed much stronger efficacy on suppressing the expression of c-Met to almost undetectable level. The c-Met suppressive effect by PTER was further validated in 231BrM, SKBrM3, and 231HM at different doses (Fig. 7C and Supplementary Fig. S7C). As we expected, the expression of IL1β, IL8, and CXCL1 was significantly suppressed in the conditioned medium prepared from PTER-treated 231BrM (Supplementary Fig. S7D). We also found that the proteasome inhibitor, MG132, did not rescue the c-Met inhibitory effect by PTER, and that c-Met mRNA expression was significantly decreased by the PTER treatment in 231BrM cells, suggesting that PTER suppresses c-Met through transcriptional regulation (Supplementary Fig. S7E and S7F). Furthermore, several previous studies have shown that PTER is able to effectively cross the BBB, and minimum local and systemic toxicity of PTER in various animal models was reported (22, 23). Therefore, to assess the efficacy of PTER in suppressing brain metastases *in vivo*, nude mice were inoculated with luciferase-labeled 231BrM cells by intracardiac injection followed by treatment with PTER (30 mg/kg/day) or vehicle alone. As shown in Fig. 7D, the PTER treatment significantly blocked the metastatic growth in the brain and increased the brain metastasis-free survival. The result of our IHC analysis also indicates

that the c-Met expression was strongly suppressed in the metastatic brain of animals that were treated with PTER compared with a control group (Supplementary Fig. S7G). We also found that treatment of PTER reduced the primary tumor growth (Supplementary Fig. S7H); however, the growth suppressive effect was significantly less striking compared to the effect on brain metastasis (3-fold vs. 100-fold reduction, respectively). Furthermore, to examine whether PTER affects perivascular attachment and angiogenesis of brain metastatic cells, 231BrM and SKBrM3 cells were treated with PTER followed by the binding assay with HBMECs. Accordingly, PTER treatment significantly attenuated the adhesion abilities of tumor cells to HBMECs (Fig. 7E). Moreover, the CM derived from PTER-treated brain metastatic cells significantly suppressed the angiogenic activity induced by the brain metastatic CM (Fig. 7F). These results suggest that PTER is a potential agent to treat brain metastases by targeting c-Met mediated perivascular growth and angiogenesis. Figure 7G illustrates c-Met signaling regulated inflammatory network in brain metastasis.

Discussion

Due to lack of a suitable biomarker for an early detection and effective therapeutic approach, brain metastasis is becoming a major health threat to the breast cancer patients. In this report, to identify genes that drive the pathological process of brain metastasis, we developed a screening approach consisting of a GSEA-based pathway analysis followed by a brain metastasis-free survival analysis. This approach is more informative and comprehensive than simply comparing the brain metastasis-free survival among each candidate gene because the latter may include many redundancies of common pathways. Using this unique approach, we found that c-Met signaling is the most frequently activated brain metastasis-associated pathway and that its expression was significantly correlated with a poor brain metastasis-free survival. Our results suggest that c-Met^{high} cells in the tumor will first generate HGF-rich environment by auto-activating IL1β followed by inducing HGF production from the TAAs, which then activates c-Met signaling in the other c-Met^{low} cells. This scenario may also explain the long latent period of brain metastasis. Therefore, blocking this vicious cycle created by metastatic cells at the brain microenvironment is considered to be an effective therapeutic approach.

Pericytes, astrocytes, and brain microvascular endothelial cells are the three major components of BBB. In addition to their known function as physical barrier, they also control neuron differentiation and proliferation by generating a perivascular niche (24). Metastatic tumor cells also utilize the perivascular niche to support their growth. Notably, disrupting the association of tumor cells with the niche by blocking the key adhesion molecules in cancer cells was shown to drastically lower the incidence of brain metastasis by activating their pro-apoptotic pathways (8). Interestingly, the levels of several key extracellular adhesion molecules, including CDH11, CLDN1, CTNNB1, and ICAM1, were found to be significantly decreased in tumor cells when c-Met was knocked-down (Supplementary Table S5), suggesting that c-Met signaling may systematically regulate a network of adhesion molecules to promote tumor cell survival and growth at the perivascular niche. In addition to the initial co-option with the existing blood vessels, the further outgrowth of tumor requires neoangiogenesis, which is triggered by various pro-angiogenic growth factors. In fact, Kim and colleagues previously demonstrated that the brain metastatic lesions generated by selected brain metastatic cells contained more CD31-positive blood vessels than lesions generated by the parental cells (25). We also showed that c-Met signaling significantly induced the secretion of IL8 and CXCL1. Interestingly, Garau and colleagues found that the CXCR1/2 inhibitor repertaxin is capable of crossing the BBB and prevents brain ischemia in rats, suggesting that this drug may be a potential candidate to suppress brain metastases by blocking angiogenesis at perivascular niche (26).

A large number of GFAP-positive astrocytes are often found in the brain metastatic lesions, suggesting that they play critical roles in brain metastasis (27). Interestingly, two recent published articles demonstrated apparent opposite roles of GFAP^{+} astrocytes in brain metastasis (8, 10). Our results suggest that brain metastatic cells are capable of triggering a phenotypic switch from normal astrocytes to TAAs through the IL1β-mediated NF-κB pathway. It is probable that astrocytes exert its antitumoral activity at an early stage of metastatic growth as described previously (16). However, at the later stage, they may be transformed to TAAs through reciprocal interaction with tumor cells, and this reprogramed TAA gains the ability to support the metastatic growth as we found in this study.

There are growing interests in using natural compounds or supplements as chemopreventive agents for reducing the risk of distant metastasis owing to their low toxicity. Su and colleagues recently found that PTER attenuated metastatic potential of breast cancer cells by modulating several key genes involved in epithelial mesenchymal transition (28). Therefore, the tumor suppressive functions of PTER are mediated through complex networks that are involved in the modulation of multiple key oncogenic pathways. Nevertheless, BBB permeability of PTER and its known targets in brain metastasis as revealed by this study offer this natural compound as an attractive candidate for chemoprevention or treatment for brain metastasis.

Disclosure of Potential Conflicts of Interest

M.D. Chan is a consultant/advisory board member for Novocure. No potential conflicts of interest were disclosed by the other authors.

Authors' Contributions

Conception and design: F. Xing, K. Wu, R.L. Carpenter, L.J. Metheny-Barlow, X. Zhou, K. Watabe

Development of methodology: F. Xing, S. Sharma

Acquisition of data (provided animals, acquired and managed patients, provided facilities, etc.): F. Xing, R.L. Carpenter, S.A. Qasem

Analysis and interpretation of data (e.g., statistical analysis, biostatistics, computational analysis): F. Xing, Y. Liu, M.D. Chan

Writing, review, and/or revision of the manuscript: F. Xing, S. Sharma, M.D. Chan, H.-W. Lo, L.J. Metheny-Barlow, X. Zhou, B. Pasche, K. Watabe

Administrative, technical, or material support (i.e., reporting or organizing data, constructing databases): F. Xing, Y. Liu, K. Wu, K. Watabe

Study supervision: F. Xing, K. Watabe

Acknowledgments

We thank Dr. Joan Massagué and Dr. Shizhen (Emily) Wang for providing the brain metastatic cell lines.

Grant Support

This work was supported by NIH grant R01CA173499 and R01CA185650 (K.W), a pilot grant from Comprehensive Cancer Center of Wake Forest University (F. Xing). The Tumor Tissue and Pathology Shared Resources,

Biostatistics/Bioinformatics Shared Resource are supported by the Comprehensive Cancer Center of Wake Forest University NCI, National Institutes of Health Grant (P30CA012197).

The costs of publication of this article were defrayed in part by the payment of page charges. This article must therefore be hereby marked *advertisement* in accordance with 18 U.S.C. Section 1734 solely to indicate this fact.

Received January 4, 2016; revised June 15, 2016; accepted June 20, 2016; published OnlineFirst June 30, 2016.

References

1. Maher EA, Mietz J, Arteaga CL, DePinho RA, Mohla S. Brain metastasis: opportunities in basic and translational research. Cancer Res 2009;69: 6015–20.
2. Siegel R, Naishadham D, Jemal A. Cancer statistics, 2013. CA Cancer J Clin 2013;63:11–30.
3. Weigelt B, Peterse JL, van 't Veer LJ. Breast cancer metastasis: markers and models. Nat Rev Cancer 2005;5:591–602.
4. Jaboin JJ, Ferraro DJ, DeWees TA, Rich KM, Chicoine MR, Dowling JL, et al. Survival following gamma knife radiosurgery for brain metastasis from breast cancer. Radiat Oncol 2013;8:131.
5. Voduc KD, Cheang MC, Tyldesley S, Gelmon K, Nielsen TO, Kennecke H. Breast cancer subtypes and the risk of local and regional relapse. J Clin Oncol 2010;28:1684–91.
6. Psaila B, Lyden D. The metastatic niche: adapting the foreign soil. Nat Rev Cancer 2009;9:285–93.
7. Fidler IJ. The pathogenesis of cancer metastasis: the 'seed and soil' hypothesis revisited. Nat Rev Cancer 2003;3:453–8.
8. Valiente M, Obenauf AC, Jin X, Chen Q, Zhang XH, Lee DJ, et al. Serpins promote cancer cell survival and vascular co-option in brain metastasis. Cell 2014;156:1002–16.
9. Kienast Y, von Baumgarten L, Fuhrmann M, Klinkert WE, Goldbrunner R, Herms J, et al. Real-time imaging reveals the single steps of brain metastasis formation. Nat Med 2010;16:116–22.
10. Zhang L, Zhang S, Yao J, Lowery FJ, Zhang Q, Huang WC, et al. Microenvironment-induced PTEN loss by exosomal microRNA primes brain metastasis outgrowth. Nature 2015;527:100–4.
11. Bos PD, Zhang XH, Nadal C, Shu W, Gomis RR, Nguyen DX, et al. Genes that mediate breast cancer metastasis to the brain. Nature 2009;459:1005–9.
12. Xing F, Kobayashi A, Okuda H, Watabe M, Pai SK, Pandey PR, et al. Reactive astrocytes promote the metastatic growth of breast cancer stem-like cells by activating Notch signalling in brain. EMBO Mol Med 2013;5:384–96.
13. Nobili S, Lippi D, Witort E, Donnini M, Bausi L, Mini E, et al. Natural compounds for cancer treatment and prevention. Pharmacol Res 2009;59:365–78.
14. Fricker G. Drug interactions with natural products at the blood brain barrier. Curr Drug Metab 2008;9:1019–26.
15. Liberzon A, Birger C, Thorvaldsdottir H, Ghandi M, Mesirov JP, Tamayo P. The Molecular Signatures Database (MSigDB) hallmark gene set collection. Cell Syst 2015;1:417–25.
16. Stein GY, Yosef N, Reichman H, Horev J, Laser-Azogui A, Berens A, et al. Met kinetic signature derived from the response to HGF/SF in a cellular model predicts breast cancer patient survival. PLoS One 2012;7:e45969.
17. Zhang XH, Wang Q, Gerald W, Hudis CA, Norton L, Smid M, et al. Latent bone metastasis in breast cancer tied to Src-dependent survival signals. Cancer Cell 2009;16:67–78.
18. Organ SL, Tsao MS. An overview of the c-MET signaling pathway. Ther Adv Med Oncol 2011;3(1 Suppl):S7–S19.
19. Carbonell WS, Ansorge O, Sibson N, Muschel R. The vascular basement membrane as "soil" in brain metastasis. PLoS One 2009;4:e5857.
20. Lawrence T. The nuclear factor NF-kappaB pathway in inflammation. Cold Spring Harb Perspect Biol 2009;1:a001651.
21. Surh YJ. Cancer chemoprevention with dietary phytochemicals. Nat Rev Cancer 2003;3:768–80.
22. Zhou Y, Zhang XM, Ma A, Zhang YL, Chen YY, Zhou H, et al. Orally administrated pterostilbene attenuates acute cerebral ischemia-reperfusion injury in a dose- and time-dependent manner in mice. Pharmacol Biochem Behav 2015;135:199–209.
23. Ruiz MJ, Fernandez M, Pico Y, Manes J, Asensi M, Carda C, et al. Dietary administration of high doses of pterostilbene and quercetin to mice is not toxic. J Agric Food Chem 2009;57:3180–6.
24. Abbott NJ, Ronnback L, Hansson E. Astrocyte-endothelial interactions at the blood-brain barrier. Nat Rev Neurosci 2006;7:41–53.
25. Kim LS, Huang S, Lu W, Lev DC, Price JE. Vascular endothelial growth factor expression promotes the growth of breast cancer brain metastases in nude mice. Clin Exp Metastasis 2004;21:107–18.
26. Garau A, Bertini R, Mosca M, Bizzarri C, Anacardio R, Triulzi S, et al. Development of a systemically-active dual CXCR1/CXCR2 allosteric inhibitor and its efficacy in a model of transient cerebral ischemia in the rat. Eur Cytokine Netw 2006;17:35–41.
27. Fitzgerald DP, Palmieri D, Hua E, Hargrave E, Herring JM, Qian Y, et al. Reactive glia are recruited by highly proliferative brain metastases of breast cancer and promote tumor cell colonization. Clin Exp Metastasis 2008;25:799–810.
28. Su CM, Lee WH, Wu AT, Lin YK, Wang LS, Wu CH, et al. Pterostilbene inhibits triple-negative breast cancer metastasis via inducing microRNA-205 expression and negatively modulates epithelial-to-mesenchymal transition. J Nutr Biochem 2015;26:675–85.